Journal of Magnetic Resonance 207 (2010) 274–282

Contents lists available at ScienceDirect

Journal of Magnetic Resonance

journal homepage: www.elsevier.com/locate/jmr

Numerical simulations of short-mixing-time double-wave-vector diffusion-weighting experiments with multiple concatenations on whole-body MR systems

Jürgen Finsterbusch *

Department of Systems Neuroscience, University Medical Center Hamburg–Eppendorf, Hamburg, Germany
Neuroimage Nord, University Medical Centers Hamburg–Kiel–Lübeck, Germany

ARTICLE INFO

Article history:
Received 12 May 2010
Revised 14 September 2010
Available online 19 September 2010

Keywords:
Double-wave-vector diffusion weighting
Multiple-wave-vector diffusion weighting
Multiple concatenations
Restricted diffusion
Cell size
Pore size

ABSTRACT

Double- or two-wave-vector diffusion-weighting experiments with short mixing times in which two diffusion-weighting periods are applied in direct succession, are a promising tool to estimate cell sizes in the living tissue. However, the underlying effect, a signal difference between parallel and antiparallel wave vector orientations, is considerably reduced for the long gradient pulses required on whole-body MR systems. Recently, it has been shown that multiple concatenations of the two wave vectors in a single acquisition can double the modulation amplitude if short gradient pulses are used. In this study, numerical simulations of such experiments were performed with parameters achievable with whole-body MR systems. It is shown that the theoretical model yields a good approximation of the signal behavior if an additional term describing free diffusion is included. More importantly, it is demonstrated that the shorter gradient pulses sufficient to achieve the desired diffusion weighting for multiple concatenations, increase the signal modulation considerably, e.g. by a factor of about five for five concatenations. Even at identical echo times, achieved by a shortened diffusion time, a moderate number of concatenations significantly improves the signal modulation. Thus, experiments on whole-body MR systems may benefit from multiple concatenations.

1. Introduction

In double-wave-vector diffusion weighting (DWV) [1–4] two diffusion-weighting periods are applied successively in a single experiment. This combination allows the investigation of the correlation of the spins' diffusion, e.g. in time or in different spatial directions. It can offer access to microscopic properties of the sample [1–4] if the additional degrees of freedom provided, the relative angle and the mixing time between the two diffusion weightings, are exploited. For long mixing times, diffusion anisotropy present on a microscopic level can be detected as a signal difference between parallel and orthogonal wave vector orientations even if the sample macroscopically appears isotropic [3–9]. At short mixing times, a signal difference is expected between a parallel and an antiparallel wave vector orientation in the presence of restricted diffusion [3], i.e. the signal amplitude differs between acquisitions with the two diffusion weightings in the same and in opposite directions. This difference has been shown to be proportional to a measure of the cell or pore size, the mean-squared radius of gyration, if the diffusion is fully restricted and short gradient pulses are assumed [3].

The signal modulation present at short mixing times has been observed experimentally in a variety of samples, e.g. water between beads [10], plant tissue [10], *ex vivo* spinal cord [10,11], and water in microcappilaries [12–14], and recently has also been reported for the cortico-spinal tract in the living human brain [15,16]. However, the signal differences present in experiments on clinical whole-body MR systems are quite small, typically only a few percent [10]. Analytical calculations [17] and numerical simulations [18] have shown that the signal difference decreases considerably for the gradient pulse duration required to achieve a sufficient diffusion weighting on whole-body MR systems. For instance, for gradient pulses of 20 ms, it is reduced by about a factor of 16 for ellipsoidal cells with an average diameter of 5 μm [18]. This decrease hampers the reliable and accurate determination of the signal difference on clinical MR systems.

Recently, an extension of the DWV experiment was presented that involves multiple concatenations of the two wave vectors [19,20], i.e. more than two diffusion weightings are applied successively and alternate between the two wave vectors. It has been shown theoretically and in numerical simulations that this

* Address: Institut für Systemische Neurowissenschaften, Geb. W34, Universitätsklinikum Hamburg-Eppendorf, 20246 Hamburg, Germany. Fax: +49 40 7410 59955.
E-mail address: j.finsterbusch@uke.uni-hamburg.de

1090-7807/$ - see front matter © 2010 Elsevier Inc. All rights reserved.
doi:10.1016/j.jmr.2010.09.009

approach increases the modulation amplitude at short mixing times by up to a factor of two, which can help to improve the detectability of the underlying effect [19]. However, these results were obtained within the short-pulse-approximation and for long diffusion times, i.e. effectively fully restricted diffusion.

In this study, numerical simulations of DWV experiments with multiple concatenations at short mixing times were performed for gradient pulse durations and timing parameters compatible with standard whole-body MR experiments. It is shown that the derived tensor model [19,21] still yields a good approximation of the simulated data if an additional term is included. This term describes free, anisotropic diffusion and can be considered to represent spins within the fully restricted compartment that, for the finite timing parameters used, do not contribute to the signal modulation, i.e. show the signal behavior of freely diffusing spins. More importantly, it is demonstrated that the gain of the modulation amplitude obtained with multiple concatenations is considerably higher than expected if the higher diffusion-weighting efficiency of multiple concatenations is used to shorten the pulse durations. Thus, multiple concatenations may help to improve the detectability of the DWV effect at short mixing times, in particular on whole-body MR systems.

2. Theory

The tensor model presented for the generalized experiment with multiple concatenations (Fig. 1) [19] is summarized in the following paragraphs. It is based on the assumptions that the mixing time and the gradient pulse durations are short ($\tau_m, \delta \to 0$) and the diffusion time Δ is long compared to $\tau_D = \frac{a^2}{2D}$ (with the pore diameter a and the diffusion coefficient D), i.e. the time a spin typically needs to cross the pore.

Then, the signal expression for arbitrary wave vectors, pore sizes, and pore size orientation distributions and n concatenations is given by [19,21]

$$M_n(\mathbf{Q}) \propto 1 - \frac{1}{2}\mathbf{Q}^T \underline{\underline{\mathbf{T}}}_n \mathbf{Q} \tag{1}$$

with $\mathbf{Q} = (\mathbf{q}_1{}^T, \mathbf{q}_2{}^T)^T$ being composed of the two wave vectors $\mathbf{q}_i = \gamma\delta\mathbf{G}_i$ (γ: gyromagnetic ratio, $\mathbf{G}_i$: gradient amplitude). $\underline{\underline{\mathbf{T}}}_n$ is a 6×6 tensor given by [19]

$$\underline{\underline{\mathbf{T}}}_n = \begin{pmatrix} 2n\underline{\underline{\mathbf{R}}} & (2n-1)\underline{\underline{\mathbf{R}}} \\ (2n-1)\underline{\underline{\mathbf{R}}} & 2n\underline{\underline{\mathbf{R}}} \end{pmatrix} \tag{2}$$

or

$$\underline{\underline{\mathbf{T}}}_n = \begin{pmatrix} (2n'+1)\underline{\underline{\mathbf{R}}} & (2n'-1)\underline{\underline{\mathbf{R}}} \\ (2n'-1)\underline{\underline{\mathbf{R}}} & (2n'-1)\underline{\underline{\mathbf{R}}} \end{pmatrix} \tag{3}$$

for an even (Fig. 1a) and an odd number of diffusion weightings (Fig. 1b, $n' = n + \frac{1}{2}$), respectively, and is based on the elements of the 3×3 tensor $\underline{\underline{\mathbf{R}}}$. They are defined by

$$R_{ij} = \int_{\text{pore}} \rho(\mathbf{r}) r_i r_j \, d\mathbf{r} \tag{4}$$

where $\rho(\mathbf{r})$ is the spin density distribution within the pore. If only the signal difference between the parallel and antiparallel wave vector orientation is considered,

$$\Delta M(\mathbf{q}) = \mathbf{q}^T 2(2n-1)\, \underline{\underline{\mathbf{R}}}\mathbf{q} \tag{5}$$

is obtained where $q = q_1 = q_2$ was assumed. For an isotropic orientation distribution of the pores, Eq. (1) yields

$$M_{\text{iso}}(\mathbf{q}_1, \mathbf{q}_2) \propto 1 - \frac{1}{3}\rho\, q^2 \langle R^2 \rangle \, (2n + (2n-1)\cos\theta) \tag{6}$$

for $q = q_1 = q_2$ where θ is the angle between the two wave vectors and $\langle R^2 \rangle$ the mean-squared radius of gyration defined by [3]

$$\langle R^2 \rangle = \int_{\text{pore}} \rho(\mathbf{r}) r^2 d\mathbf{r} \tag{7}$$

Thus, $\langle R^2 \rangle = \sum_i R_{ii}$, i.e. it is the trace of the tensor $\underline{\underline{\mathbf{R}}}$. In case of an odd number of diffusion weightings (Fig. 1b), n in Eqs. (5) and (6) must be replaced by $n' = n + \frac{1}{2}$.

For an isotropic orientation distribution, the modulation amplitude increases with the number of concatenations, as can be seen in Eq. (6). For instance, for constant $n \cdot q^2$, i.e. a fixed diffusion weighting, the relative modulation amplitude is given by $1 - \frac{1}{2n}$. This means that it increases with the number of concatenations, but at most is doubled in the limit of large n.

In the presence of freely diffusing spins Eqs. (1) and (6) must be adapted. Eq. (5) remains valid because there is no signal difference between parallel and antiparallel wave vector orientations for free diffusion. In Eq. (6), an additional second order term $-D4nq^2\Delta$ (for $q_1 = q_2 = q$) with the free diffusion coefficient D must be added, which is obtained from the Taylor expansion of the exponential signal decay present for free diffusion. Thus, the free diffusion term, re-written as a function of $\mathbf{Q}$, is given by

$$M_{\text{free}}(\mathbf{Q}) \propto 1 - 2n\Delta D \mathbf{Q}^T \begin{pmatrix} \underline{\underline{\mathbf{1}}} & 0 \\ 0 & \underline{\underline{\mathbf{1}}} \end{pmatrix} \mathbf{Q}. \tag{8}$$

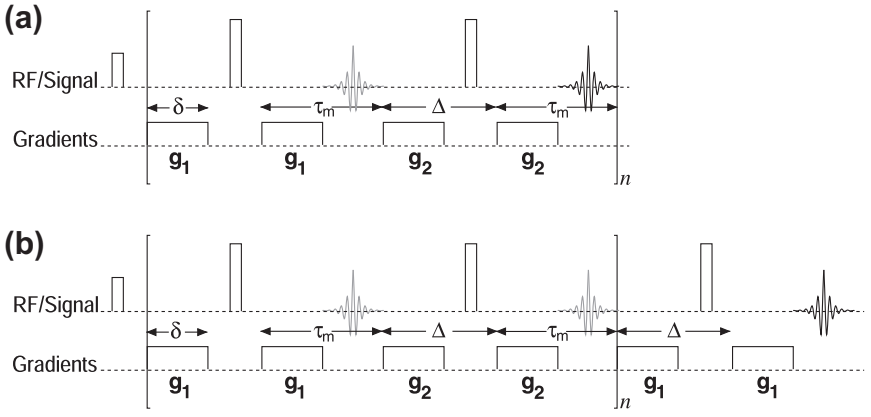

Fig. 1. Basic pulse sequences for the double-wave-vector (DWV) diffusion-weighting experiments with multiple concatenations of the two wave vectors investigated in the current study. (a) n concatenations with an even number of diffusion weightings, (b) $n' = n + \frac{1}{2}$ concatenations with an odd number of diffusion weightings, i.e. a final diffusion weighting using the first wave vector. Note that the diffusion weightings shown represent a parallel orientation of the two wave vectors according to the notation introduced in [3], i.e. the rephasing gradient of the first diffusion weighting has the same polarity as the dephasing pulse of the second one.

In the more general case of anisotropic diffusion, this expression must be extended to

$$M_{\underline{\underline{\mathbf{D}}}}(\mathbf{Q}) \propto 1 - 2n\ \Delta\mathbf{Q}^T \begin{pmatrix} \underline{\underline{\mathbf{D}}} & 0 \\ 0 & \underline{\underline{\mathbf{D}}} \end{pmatrix} \mathbf{Q} \tag{9}$$

where $\underline{\underline{\mathbf{D}}}$ is the well-known (second order) diffusion tensor with $D = \frac{1}{3}\mathrm{Tr}(\underline{\underline{\mathbf{D}}})$. As before, $2n$ must be replaced by $2n' = 2n + 1$ for a half-integral number of concatenations (Fig. 1b), i.e. an odd number of diffusion weightings.

In this study, only spins in a fully restricted compartment, spherical or ellipsoidal pores or cells with impermeable boundaries, were simulated. Nevertheless, terms according to Eqs. (8) and (9) describing free diffusion were included in the model to account for the finite timing parameters used. For instance, for a finite diffusion time, there are spins that will not reach the walls, i.e. will not "feel" the restrictions, and, thus, will behave like freely diffusing spins on the time scale of the experiment. In the DWV experiment, such spins will not show the expected signal modulation with the relative angle between the two wave vectors. The finite gradient pulse durations and mixing times used in real experiments can cause similar effects. The signal difference between parallel and antiparallel wave vector orientations is based on the correlation of the displacements occurring during the two successive diffusion weightings. Spins that have moved to one, e.g. the left, boundary during the first diffusion weighting cannot diffuse further in this direction during the second diffusion weighting but effectively will move away in the other, i.e. the right, direction and vice versa. However, if the mixing time is long enough, fast spins have time to diffuse to anywhere within the pore before the next diffusion weighting starts. This means that the correlation is lost for these spins and that they will not contribute to the expected signal modulation as well. To account for such effects, the free diffusion terms can be added to the model. The expression "apparently free" will be used for corresponding signal contributions.

The amount of apparently free spins depends on the size of the pores or cells for given timing parameters. For instance, more spins will fail to reach the walls for large pores. This means that for non-spherical pores or cells, the effect will depend on the direction of the diffusion weighting. Thus, the free diffusion term of Eq. (9) that takes a direction dependency into account, seems to be more appropriate in general as will be demonstrated in Section 4. However, if an isotropic orientation distribution of the pores is considered, the isotropic variant, i.e. Eq. (8), is sufficient.

Mathematically, and more generally, the additional term is introduced to model deviations from the tensor equations observed in experiments with finite timing parameters. This means, for instance, that it can not only describe the extreme cases described above (spins that never "see" the walls or show a complete loss of the correlation between the two diffusion weightings), but it will cover any reduction in the signal modulation amplitude caused, e.g., by a violation of the assumptions underlying the tensor model: fully restricted diffusion ($\Delta \to \infty$), perfect correlation ($\tau_m \to 0$), and instantaneous diffusion en- and decoding ($\delta \to 0$).

It should be noted that the additional term represents a simple, phenomenological approach to consider deviations from the tensor model. In particular, it is needed to model the mean signal decay independently from the signal modulation. Because only the signal difference but not the signal decay is analyzed to estimate pores sizes, a more elaborated derivation is not needed.

3. Experimental

Numerical simulations of the MR signal in DWV experiments were performed and analyzed with a self-written IDL algorithm (version 7.0, ITT Visual Information Solutions, Boulder, Colorado, USA) as described previously [19,21]. Spins were simulated in a single, fully restricted compartment. Spherical pores with radii between 2.5 μm and 10 μm and prolate ellipsoidal pores with semi-principal axes (short/long axis) of 2.5/5.0 μm and 1.0/4.0 μm, respectively, were considered, both with impermeable boundaries. The random walk of 10000 spins within the pore was considered with a temporal resolution of 10 μs and a diffusion coefficient of 2.0×10^{-3} mm^2 s^{-1}. This yields τ_D values with maxima of 100 ms, 25 ms, and 16 ms and minima of 6 ms, 6 ms, and 1 ms for the spheres and the ellipsoids' long and short axes, respectively. Between one and six concatenations (n) were considered, for experiments with a half-integral number of concatenations n' values of $\frac{3}{2}$ and $\frac{5}{2}$ were used corresponding to one and two full cycles, respectively, plus the terminating diffusion weighting (Fig. 1b). Identical magnitudes of the two wave vectors were assumed in all simulations ($q_1 = q_2 = q$).

A minimum τ_m of δ was used in the simulations for two reasons. First, the b value of the diffusion weighting depends on the relative angle between the two wave vectors for $\tau_m < \delta$ which can add an extra signal modulation, e.g. for (apparently) free spins, that may mask the restriction effect. Second, the simulations focussed on the signal characteristics for the limited maximum gradient amplitude ($G_{\max}$) available on whole-body MR systems. For $\tau_m \geqslant \delta$, two successive gradient pulses of amplitude $g_1 = g_2 = G_{\max}$ (see e.g. Fig. 1a) can be used, but for $\tau_m < \delta$, the pulses overlap and $g_1 = g_2 = \frac{1}{2}G_{\max}$ is required, which means that the pulse durations need to be doubled to reach the desired diffusion weighting.

For the first wave vector, 1651 orientations distributed over a sphere were considered as described previously [21]. For the second wave vector, 3302 directions were used that were obtained from the directions of the first wave vector plus their antipodes in order to ensure a sufficiently dense sampling of both, the parallel and antiparallel wave vector orientations.

Two different strategies were used to analyze the simulation results. The first used the average signal from all wave vector combinations that, rounded to an accuracy of five degrees, enclosed the same angle. Using this approach, the signal for an isotropic orientation distribution of the pores is obtained and can be fitted to Eq. (6) to estimate the mean-squared radius of gyration. Note that this implies that each of the $1651 \times 3302 = 5.45$ million direction combinations simulated contributed to one of the $360°/5° = 72$ sampling points of the mean curve. Signal contributions from apparently free spins were considered according to Eq. (8) in this case. In the second strategy, each wave vector combination was considered as an individual measurement and either all of these combinations or only those with parallel and antiparallel orientations were fitted by Eqs. (1) and (5) to determine the elements of $\underline{\underline{\mathbf{R}}}$ and $\underline{\underline{\mathbf{T}}}_n$, respectively. Here, Eq. (9) was included in the fit procedure. For both strategies, a Levenberg–Marquardt algorithm as described in [22] was used for the fit.

The number of particles simulated (10,000) was constrained by the large data amount and long calculation times of multiple concatenations and limits the reproducibility and accuracy of the simulations, in particular for ellipsoidal pores. In spherical pores, a random preference of the simulated paths into a specific direction does not affect the signal difference because it does not depend on the direction. In ellipsoidal pores, however, such a preference yields a higher signal modulation if it is along the long axis of the ellipsoid compared to cases where it coincides with the short axis. To estimate the related uncertainty, eight different simulations were performed for ellipsoids with semi-axes of 1/4 μm for q values from 173 mm^{-1} to 403 mm^{-1} and different numbers of concatenations. The maximum standard deviations observed in these simulations was about 0.15% of the signal intensity without diffusion weighting.

Simulations were performed for a whole-body MR system (maximum gradient amplitude 40 mT m^{-1}) and a research-dedicated gradient insert (maximum gradient amplitude 80 mT m^{-1}) [23]. Thereby, it was assumed that two axis are applied simulatenously which is compatible with sampling parallel, antiparallel, and orthogonal wave vector combinations in any plane and determining a roationally invariant measure of the effective pore size [21].

4. Results

In the first part, the influence of finite timing parameters (δ, Δ, and τ_m) on the signal modulation was investigated for the standard experiment ($n = 1$). Furthermore, the improvement of the fit upon including apparently free spins into the model is demonstrated. The corresponding results, all obtained for a constant q, are shown in Fig. 2. The signal curves simulated for a variation of the gradient pulse duration δ are presented in Fig. 2a and b. For a minimum δ, the signal curve is in good agreement with Eq. (6) for $n = 1$ which is indicated by the fit line (Fig. 2a). In particular, and as expected, the signal decay for the parallel orientation is almost three times that found for the antiparallel orientation. Some minor deviations are observed for the fit curve that increase with q (data not shown) and, thus, can be assigned to higher order signal contributions which are not considered in the model. With increasing δ, the overall signal decay as well as the modulation amplitude are decreased.

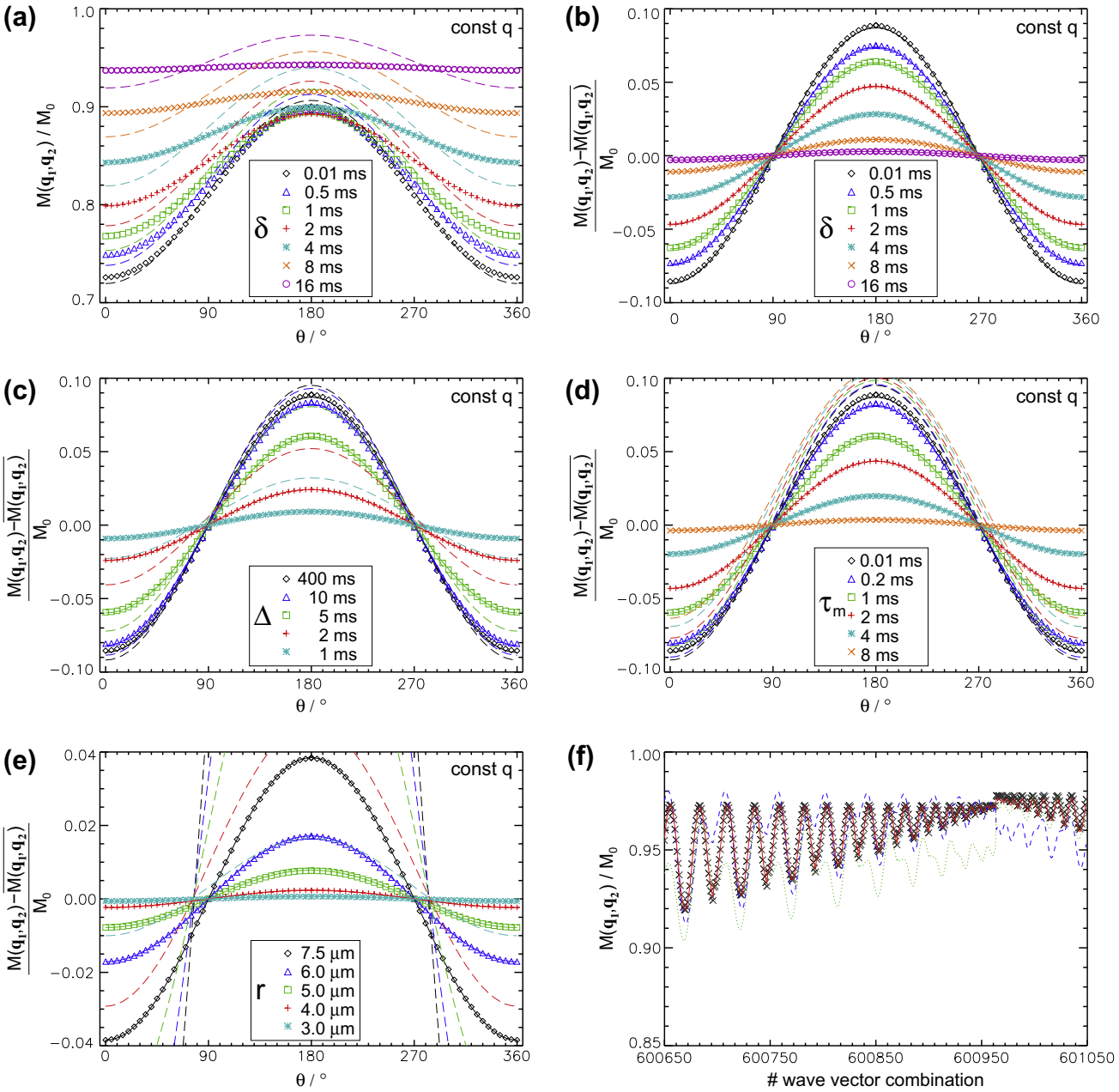

Fig. 2. Results of the MR signal simulations (symbols) and model fits (lines) for a standard experiment ($n = 1$) demonstrating the improved signal modeling achieved with the additional term describing apparently free spins. (a–e) were obtained for spherical cells with (a–d) a radius of 5 µm and (f) for ellipsoidal cells with semi-axes of 5.0, 2.5, and 2.5 µm. Different (a and b) gradient pulse durations ($\tau_m = \delta$, $\Delta = 400$ ms), (c) diffusion times Δ ($\delta = \tau_m = 0.01$ ms), (d) mixing times τ_m ($\delta = 0.01$ ms, $\Delta = 400$ ms), and (e) cell radii ($\delta = \tau_m = 20$ ms, $\Delta = 30$ ms) were considered. (f) 400 (of 5.45 millions) wave vector orientation combinations investigated for ellipsoidal cells with semi-axes of 5.0, 2.5, and 2.5 µm ($\delta = \tau_m = 20$ ms, $\Delta = 30$ ms). The lines in (a–f) represent the fits to the model without (dashed) and with (solid) the additional term. The dotted line in (f) was obtained with an additional isotropic signal contribution according to Eq. (8). q was constant in all simulations shown. Note that (b–e) show the signal modulation shifted by the mean signal value.

Thereby, the signal modulation is relatively more reduced compared to the overall signal decay yielding considerable deviations from the model fits based on Eq. (6). Considering signal contributions of apparently free spins in the fit procedure according to Eq. (8) results in a much better approximation of the simulations (Fig. 2b), even for very long δ. A similar decrease of the modulation amplitude and the signal decay and improvement of the fit is obtained in case of shorter diffusion times Δ (Fig. 2c). Using finite mixing times τ_m the effects are even more pronounced as only with the additional term can the reduced signal modulation be modeled (Fig. 2d).

While Fig. 2b–d showed examples where only one of the parameters had a non-optimal value, simulations investigating the combined effect, i.e. with realistic values for all three parameters, are presented in Fig. 2e for spherical pores with different sizes. It demonstrates the good approximation of the data by the fits with the additional term. Thereby, the fraction of the spins that are described by the additional term, i.e. appear free on the time scales of the experiments, increases with the cell radius which is consistent with the view that in larger cells more spins do not "feel" the restrictions, e.g. within the same diffusion time. This has implications for a non-isotropic orientation distribution of non-spherical pores as shown in Fig. 2f for ellipsoids and a range of wave vector orientations. Ignoring the free diffusion term does not yield a good fit (dashed), as expected, but no crucial improvement is achieved when including Eq. (8) (dotted). This is because the effect on the signal is larger along the long axis of the ellipsoid and smaller along the other directions. Thus, an isotropic contribution underestimates the apparently free contributions along the long axis and overestimates them along the shorter axes, which yields significant deviations from the simulated data. For an anisotropic term according to Eq. (9), however, a good agreement of the model with the data is obtained (solid). As a consequence, all fits of non-isotropic orientation distributions were performed with such an anisotropic signal contribution.

These results show that for finite timing parameters a better approximation of the data is achieved if apparently free spins, with in general anisotropic diffusion, are included in the tensor model. In the second part, the focus is on simulations performed with constant gradient amplitudes applicable on whole-body MR systems in order to investigate the improvements achievable with multiple concatenations. This part starts with a detailed comparison of the standard experiment with multiple concatenations to demonstrate the basic differences.

In Fig. 3a and b, series of simulations are shown that were performed for a range of gradient pulse durations at constant amplitude for a single (Fig. 3a) and five concatenations (Fig. 3b), respectively. When starting with short δ, the signal modulation first increases, achieves a maximum, i.e. an optimum pulse duration, and then decays again for longer pulse durations in both cases. This observation is consistent with previous results [18]. However, for five concatenations, the maximum is observed at a much shorter gradient pulse duration (8 ms) than for a single concatenation (16 ms).

This fact adds an additional benefit to the experiment with multiple concatenations that has not been considered so far and is demonstrated in Fig. 3c. For the standard experiment, the modulation amplitude is quite low with a maximum difference of about 1.7% (diamonds). Using five concatenations with identical diffusion weighting, i.e. at the same $n \cdot q^2$, but without changing δ, yields an increase to about 2.7% (squares). This gain is in agreement with the factor of $(1-\frac{1}{10})/(1-\frac{1}{2}) = \frac{9}{5}$ that is expected theoretically in the limit of short gradient pulse durations [19]. However, δ can be reduced by a factor of $\frac{1}{\sqrt{5}}$ for the given diffusion weighting by using the same maximum gradient amplitude as in the standard experiment ($*$). This yields a considerably higher modulation amplitude of more than 10% that is about six times higher than that of the simple experiment and almost four times higher than for a constant δ. It is even higher than the modulation amplitude observed for a constant q at unchanged δ (triangles), i.e. where the diffusion weighting of the experiment with concatenations is increased by a factor of five. It should be emphasized that this increase is only observed if the mixing time is fixed to δ. Reducing δ without shortening τ_m results in a pronounced decrease of the modulation amplitude much below that of a simple experiment (+).

The gain observed for $\tau_m = \delta$ increases with the number of concatenations as shown in Fig. 3d (at constant gradient amplitude); even for just two concatenations the signal modulation is more than doubled. Thus, it seems that experiments with multiple concatenations may benefit much more than expected from the considerations performed previously.

Also for multiple concatenations, the tensor model that takes signal contributions of apparently free spins into account is in good agreement with the signal curves. This is demonstrated for arbitrary wave vector orientation combinations (Fig. 3e) and the signal difference between parallel and antiparallel wave vector orientations (Fig. 3f). The higher modulation amplitude described above is also obvious in Fig. 3f. It is not fully present in Fig. 3e because it covers orientations combinations with lower angles between the two wave vectors while the maximum modulation is only observed if parallel and antiparallel orientations are present.

Thus, the applicability of the tensor model extended by contributions from apparently free spins has been demonstrated. In the next part, it is investigated how the improved signal modulation achieved with multiple concatenations depends on the cell or pore size and the diffusion weighting. Therefore, in the remaining simulations, a constant gradient amplitude is used and n concatenations at the same diffusion weighting were obtained by shortening the pulse duration δ according to $\frac{1}{\sqrt{n}}$.

Fig. 4 shows examples of the modulation amplitude for different numbers of concatenations and several pore or cell sizes. In all plots, multiple concatenations yield, usually considerably, higher modulations. In particular, the gain achieved is almost always well above the theoretically expected level for short gradient pulses (dashed lines, extrapolated from the simulations with $n = 1$). Exclusively, for larger cells (radius 10 μm, Fig. 4a) at high values of $n \cdot q^2$, there is only a minor gain present. However, this is due to the fact that in this size range, the signal decay is quite pronounced yielding maximum and minimum signals that approach or practically are zero, which consequently limits the observable modulation amplitude. For smaller cells, e.g. ellipsoidal cells with semi-axes of 1.0, 1.0, and 4.0 μm (Fig. 4d), the signal modulation for only a few concatenations approaches 2% with standard whole-body parameters, which can be considered to be detectable with current MR systems [18]. The maximum signal modulations clearly visible in Fig. 4a and b again reflect the optimum pulse durations as already seen in Fig. 3a and b. The gain of the signal difference beyond the theoretically expected level for short gradient pulses directly improves the pore size estimates. For instance, the mean-squared radius of gyration estimated from the curves in Fig. 4c for a $\sqrt{n}q$ of 58 mm^{-1} is only 30% of the nominal value for a simple experiment ($n = 1$) but 58% for six concatenations.

In Fig. 5a, the signal modulation for a constant gradient amplitude and diffusion weighting is plotted vs. the radius of spherical cells. It demonstrates that a considerable improvement is observed for multiple concatenations over a large range of sizes. But Fig. 5a, as Figs. 3 and 4, was obtained with identical timings of the diffusion weighting, i.e. effectively longer echo times for multiple concatenations. In contrast, Fig. 5b and c show the results of simulations where the diffusion time for multiple concatenations was shortened such that the echo time remained constant, i.e. yielding identical signal losses related to transverse relaxation.

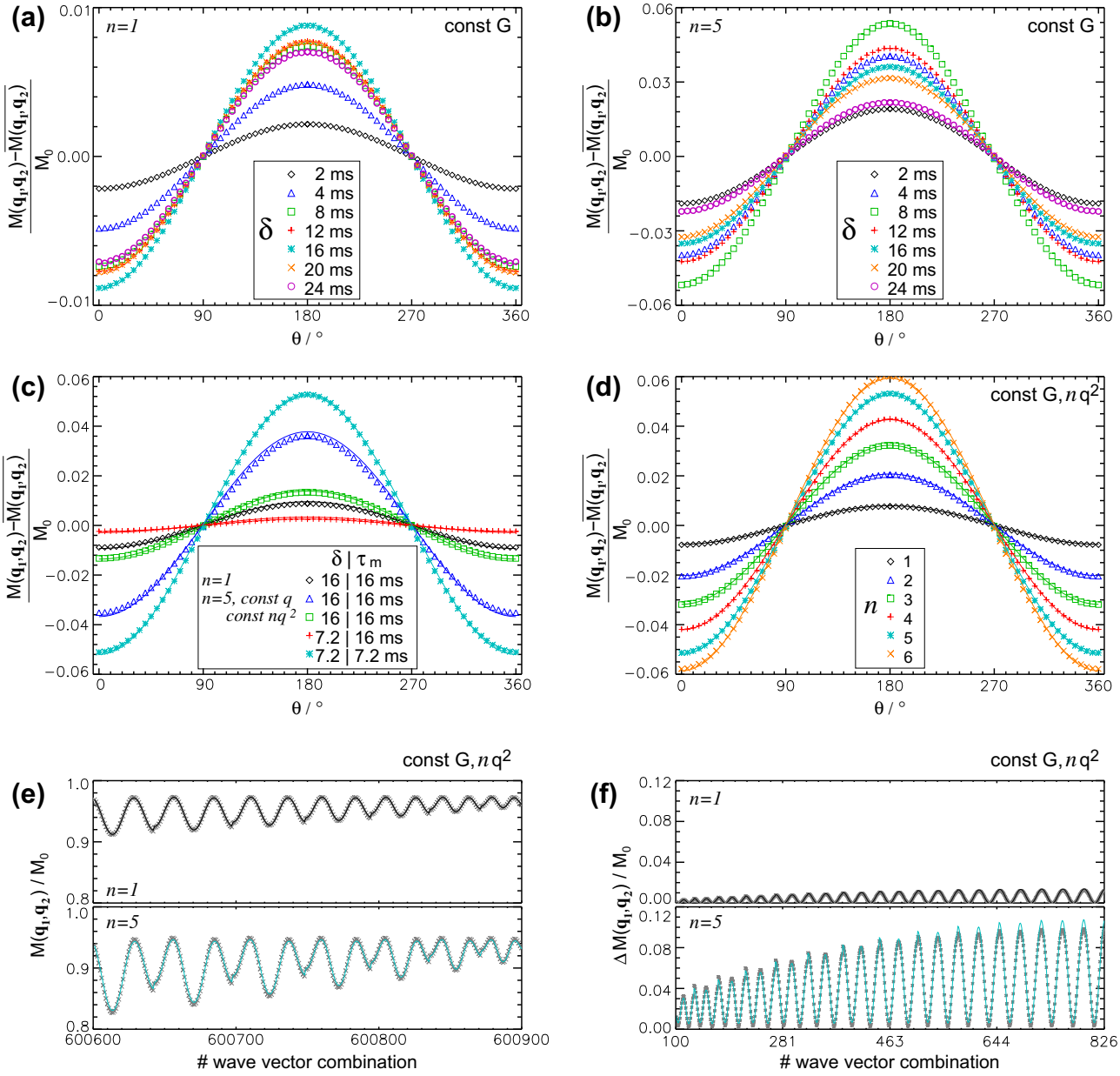

Fig. 3. Results of the MR signal simulations (symbols) and corresponding fits (lines) demonstrating the improved signal modulation for multiple concatenations. (a–d) spherical (radius 5 μm) and (e and f) ellipsoidal cells (semi-axes of 5, 2.5, 2.5 μm). (a and b) One and five concatenations, respectively, for different pulse durations δ at a diffusion time Δ of 30 ms ($\tau_m = \delta$, constant gradient amplitude). Note the different scalings. (c) Comparison of one (diamonds) and five concatenations (other symbols) with identical q (triangles) or constant $n \cdot q^2$ (square, +, ∗). Without changing δ (squares) a minor increase of the modulation amplitude is present that is consistent with the theory derived for short gradient pulses. Shortening δ by $\sqrt{n}$, i.e. using the same gradient amplitude, without touching τ_m yields an almost constant signal curve (+), however, with $\tau_m = \delta$ a considerably higher modulation amplitude is obtained (∗). (d) Simulations with one (δ = 16 ms) to six concatenations for a constant $n \cdot q^2$ and gradient amplitude. (e) 400 (of 5.45 millions) wave vector orientation combinations and (f) the difference of parallel and antiparallel wave vector orientations for 726 different directions. Fits were performed using (a–d) Eq. (6), (e) Eq. (1), and (f) Eq. (5), respectively, with additional signal contributions according to Eq. (9).

Due to the shorter diffusion time (cf. Fig. 2c), the signal modulation for multiple concatenations is reduced compared to Fig. 5a. For large cells and more than three concatenations, it may even be lower than for the simple ($n = 1$) experiment. But for a medium number of concatenations ($\frac{3}{2}$ to 3), a significant improvement is observed over a large range of cell sizes (3–9 or 10 μm, respectively), e.g. about 90% and 110% for a radius of 6.3 μm and a n of 2 or 3, respectively. Particularly, for smaller cells, this improvement, e.g. about 190% for 4 μm at three concatenations, may be crucial for observing the effect on whole-body MR systems (Fig. 5b). However, it is obvious that the modulation for even smaller cells, although improved, is expected to be below current detection limits. With the stronger gradient systems available for research purposes, the gradient pulse durations can be further shortened, which may allow a shift of the detection limit towards smaller cells, in particular in combination with multiple concatenations. This is demonstrated with simulations performed for small cells using a gradient coil with a maximum amplitude of 80 mT m^{-1} [23] (Fig. 5c). For instance, cells with a radius of 3 μm, even for the strong gradient system, reveal a modulation of only about 0.4% which is increased to about 2.6% for six concatenations at the same echo time. Nevertheless, the applicability of DWV-based cell size estimations currently seems to be limited to a few μm on whole-body MR systems.

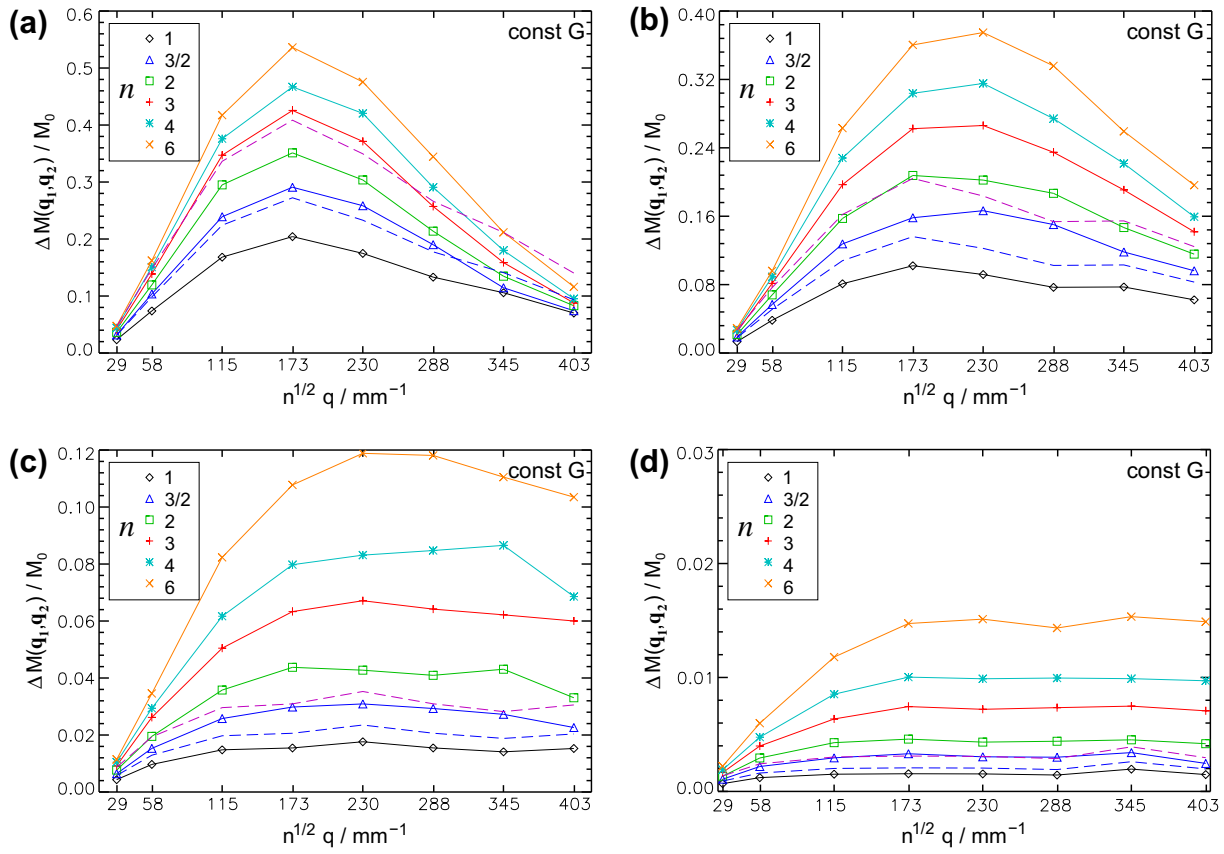

Fig. 4. Relative signal differences between parallel and antiparallel wave vector orientations vs. the diffusion weighting for different cell sizes and numbers of concatenations (Δ = 30 ms, $\tau_m = \delta$). (a–c) Spherical cells with a radius of 10.0, 7.5, and 5.0 μm, respectively, and (d) ellipsoidal cells with semi-axes of 1.0, 1.0, and 4.0 μm. A constant gradient amplitude of $\sqrt{2} \cdot 40$ mT m^{-1} was used. For a given diffusion weighting, δ was, compared to the standard experiment ($n = 1$), shortened by $1/\sqrt{n}$ for n concatenations. The dashed lines represent the signal modulation expected theoretically by extrapolating the simulations with $n = 1$ to $n = \frac{3}{2}$ (lower) and $n \to \infty$ (upper) according to Eq. (6). The curves in (c) represent averages of eight different simulations, i.e. are effectively based on 80,000 spins, to achieve a higher reliability. For details see text.

5. Discussion

In the present work, DWV experiments with short mixing times and multiple concatenations were investigated with numerical simulations for gradient pulse durations and timing parameters compatible with whole-body MR systems. It is shown that the signal can still be approximated with the equations derived for short gradient pulse durations if an additional term describing contributions from apparently free spins is added. For a given diffusion weighting, i.e. a constant $n \cdot q^2$, multiple concatenations allow shorter gradient pulse durations, which considerably increases the modulation amplitude. The gain observed in the simulations is up to four times higher than that expected from the theoretical considerations based on the assumption of short gradient pulses. Even if the same duration of the full diffusion weighting preparation is used by shortening the diffusion times for multiple concatenations appropriately, a moderate improvement can still be expected for an intermediate number of concatenations over a large range of cell sizes.

The pronounced increase of the signal modulation for multiple concatenations is related to the fact that they allow for shorter gradient pulse durations and mixing times for a given diffusion weighting. In particular for whole-body gradient coils, the standard experiment requires long gradient pulses to obtain the highest signal modulation amplitude, but thereby still loses a large part of the signal modulation that would be present in a perfect experiment with infinite short gradient pulses (cf. Fig. 2a and b). Similar observations have been reported in several previous studies, e.g. [11,12,18]. With the shorter gradient pulses sufficient for multiple concatenations, part of this loss is re-gained and adds to the theoretical benefit.

The additional (diffusion tensor) term describing anisotropic free diffusion has been added to model the reduced signal modulation present for finite gradient pulse durations and diffusion and mixing times, i.e. if the assumptions underlying the theoretical considerations are violated. It should be emphasized that this does not necessarily mean that the term completely reflects spins that do not "feel" the restrictions during the experiment. In particular, the reduction of the modulation amplitude with longer gradient pulse durations is also consistent with the signal behavior of spins undergoing restricted diffusion. For short gradient pulses, the spins' current position along the gradient direction is labeled instantaneously as a distinct phase shift that strongly varies within the cell and achieves extreme value at the cell's boundaries. For longer gradient pulses, the spins diffuse within the cell during the labeling period yielding a phase shift that has accumulated over their path during the gradient pulse. In the case of restricted diffusion, the longer the gradient pulses take, the more these paths and thus their accumulated phases converge, which reduces the crucial signal difference between parallel and antiparallel wave vector orientations. This reduction can be accounted for by assuming spins that, due to the finite timing parameters, do not show a signal modulation at all. The signal of such spins can be modeled by the additional term describing free diffusion, which also does not depend on the angle between the two wave vectors. This is consistent with the fact that the signal decay related to this

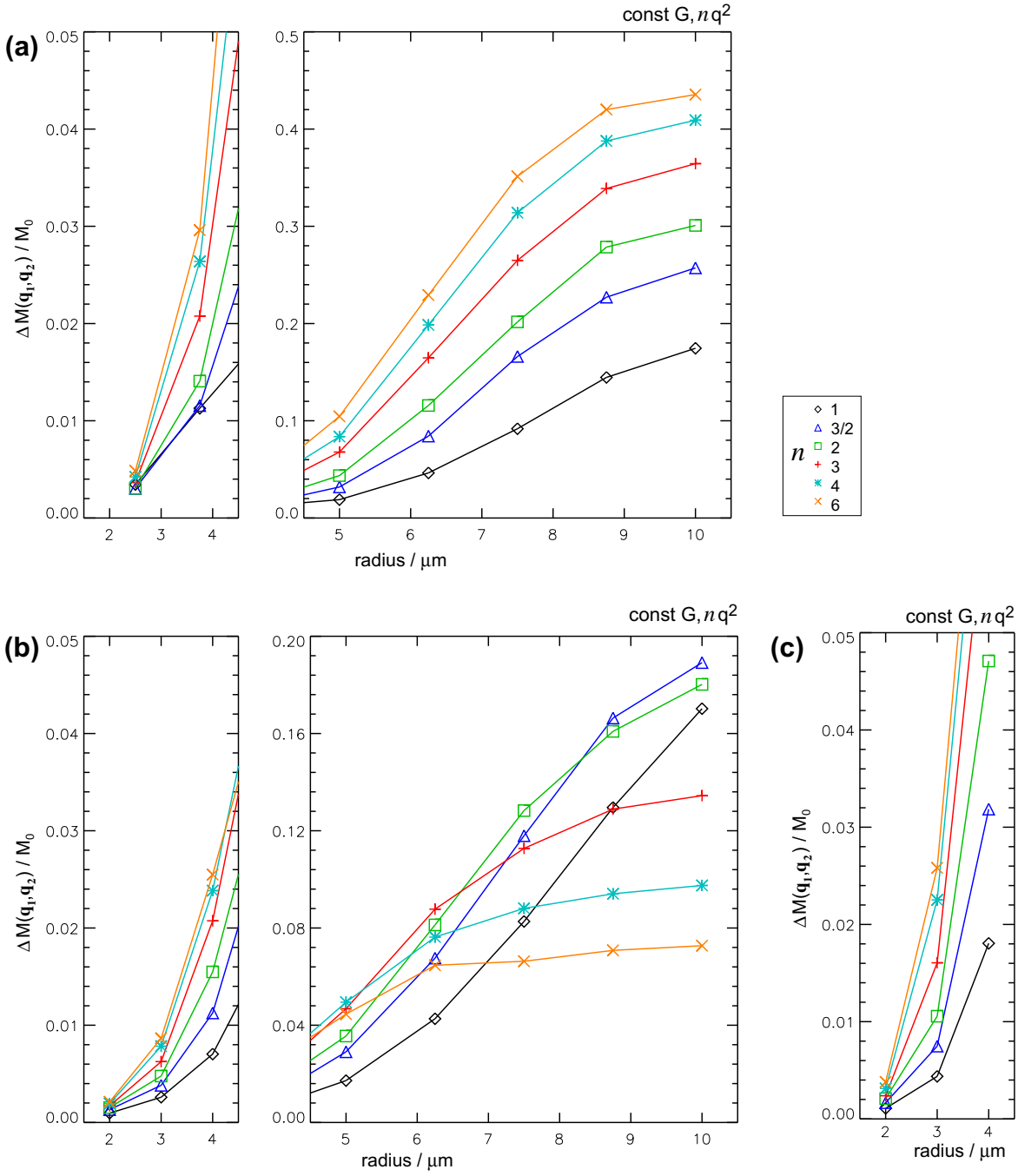

Fig. 5. Relative signal differences between parallel and antiparallel wave vector orientations vs. the cell radius of spherical cells for different numbers of concatenations with constant $\sqrt{n} \cdot q$ (230 mm^{-1}) and gradient amplitude (Δ = 30 ms, $\tau_m = \delta$). In (a), a constant timing for the diffusion weighting is considered, i.e. experiments with more concatenations need a longer echo time, in (b and c) identical echo times were obtained by shortening Δ from 30.0 ms (one concatenation) to 4.0 ms (five concatenations). (a and b) were obtained for a typical whole-body gradient system (maximum gradient amplitude 40 mT m^{-1}), (c) was simulated for a gradient coil insert with a maximum amplitude of 80 mT m^{-1} (see e.g. [23]). For n concatenations, δ was shortened by $1/\sqrt{n}$.

additional term in the simulations increased with the gradient pulse duration.

The tensor ansatz for this term may be required because the described effect depends on the cell size along the gradient direction. It reflects the most general approach in the second order of the wave vectors and thus is sufficient in the framework presented as the effect, the signal difference between parallel and antiparallel wave vectors, also appears in the second order. However, as long as isotropic orientations distributions are considered, the isotropic approach is sufficient.

The pore size estimates derived from the fits are improved for multiple concatenations, in particular if their increased diffusion weighting efficiency is used to shorten the pulse durations. However, it should be noted that although the simulation curves are well reproduced in the model including the additional term, the size estimates may still deviate significantly from the true values. This is because the spins whose signal behavior is described by the additional term are in fact not free and represent certain subpopulation of the spin ensemble, e.g. very "slow" spins that do not "feel" the restrictions within the diffusion time applied. Thus,

further refinements of the presented model or the usage of more sophisticated shape-specific models (e.g. [17]) may be desirable once the reliable detection of the signal modulation on whole-body MR systems is established.

In all simulations (except for one in Fig. 3c), the mixing time was chosen to be identical to the gradient pulse duration. Thus, it should be kept in mind that, although the simulations usually were referred to as being performed with shorter gradient pulses, the combined effect of a shorter gradient pulse and a shorter mixing time is present and influences the signal modulation (cf. Fig. 3c). However, as a short mixing time has been shown to be important for a large signal modulation, investigating the effect of artificially longer mixing times seems to be less relevant in practice.

In particular for ellipsoidal cells like that considered in Fig. 4d, some variations with $n \cdot q^2$ can be seen in the signal modulation which are in the range of the reproducability of the simulations. But this uncertainty does not affect the evidence for an improved signal modulation with multiple concatenations.

If one (Fig. 1) or two [10] refocussing RF pulse(s) are applied per diffusion weighting, the reliable suppression of unwanted signal contributions in a DWV experiment with multiple concatenations will be challenging and require large, and therefore time consuming, spoiler gradient moments on a whole-body MR system. Thus, a simpler approach, e.g. a half-integral number of concatenations (Fig. 1b) with a single refocussing RF pulse in the central diffusion-weighting period, seems to be more promising.

6. Conclusions

Double wave vector experiments with short mixing times may benefit from multiple concatenations considerably more than expected if finite timing parameters, in particular gradient pulse durations, are employed. For the shorter pulse durations that are sufficient to realize the desired diffusion weighting with multiple concatenations, the signal modulation is significantly higher with only a few concatenations, even if identical echo times are chosen. Thus, multiple concatenations may help to improve the detectability of the underlying effect, in particular on whole-body MR systems with their limited gradient amplitudes.

Acknowledgments

Parts of this study were supported by Bundesministerium für Bildung und Forschung (Neuroimage Nord).

References

[1] D.G. Cory, A.N. Garroway, J.B. Miller, Applications of spin transport as a probe of local geometry, Polym. Prepr. 31 (1990) 149–150.
[2] P.T. Callaghan, B. Manz, Velocity exchange spectroscopy, J. Magn. Reson. A 106 (1994) 260–265.
[3] P.P. Mitra, Multiple wave-vector extensions of the NMR pulsed-field-gradient spin-echo diffusion measurement, Phys. Rev. B 51 (1995) 15074–15078.
[4] P.T. Callaghan, I. Furó, Diffusion–diffusion correlation and exchange as a signature for local order and dynamics, J. Chem. Phys. 120 (2004) 4032–4038.
[5] Y. Cheng, D.G. Cory, Multiple scattering by NMR, J. Am. Chem. Soc. 121 (1999) 7935–7936.
[6] P.T. Callaghan, M.E. Komlosh, Locally anisotropic motion in a macroscopically isotropic system: displacement correlations measured using double pulsed gradient spin-echo NMR, Magn. Reson. Chem. 40 (2002) S15–S19.
[7] Y. Qiao, P. Galvosas, P.T. Callaghan, Diffusion correlation NMR spectroscopic study of anisotropic diffusion of water in plant tissues, Biophys. J. 89 (2005) 2899–2905.
[8] M.E. Komlosh, F. Horkay, R.Z. Freidlin, U. Nevo, Y. Assaf, P.J. Basser, Detection of microscopic anisotropy in gray matter and in a novel tissue phantom using double pulsed gradient spin echo MR, J. Magn. Reson. 189 (2007) 38–45.
[9] M.E. Komlosh, M.J. Lizak, F. Horkay, R.Z. Freidlin, P.J. Basser, Observation of microscopic diffusion anisotropy in the spinal cord using double-pulsed gradient spin echo MRI, Magn. Reson. Med. 59 (2008) 803–809.
[10] M.A. Koch, J. Finsterbusch, Compartment size estimation with double wave vector diffusion-weighted imaging, Magn. Reson. Med. 60 (2008) 90–101.
[11] T. Weber, C.H. Ziener, T. Kampf, V. Herold, W.R. Bauer, P.M. Jakob, Measurement of apparent cell radii using a multiple wave vector diffusion experiment, Magn. Reson. Med. 61 (2009) 1001–1006.
[12] N. Shemesh, E. Özarslan, P.J. Basser, Y. Cohen, Measuring small compartmental dimensions with low-q angular double-PGSE NMR: the effect of experimental parameters on signal decay, J. Magn. Reson. 198 (2009) 15–23.
[13] N. Shemesh, E. Özarslan, A. Bar-Shira, P.J. Basser, Y. Cohen, Observation of restricted diffusion in the presence of a free diffusion compartment: single- and double-PFG experiments, J. Magn. Reson. 200 (2009) 214–225.
[14] M.E. Komlosh, E. Özarslan, M.J. Lizak, F. Horkay, P.J. Basser, Fiber diameter mapping of a white matter phantom using d-PFG filtered MRI, in: Proceedings of the International Society for Magnetic Resonance in Medicine, 18th Annual Meeting, Stockholm, Sweden, 2010, p. 3393.
[15] M.A. Koch, J. Finsterbusch, Double wave vector diffusion weighting in the human corticospinal tract in vivo, in: Proceedings of the International Society for Magnetic Resonance in Medicine, 16th Annual Meeting, Toronto, Canada, 2008, p. 764.
[16] M.A. Koch, J. Finsterbusch, In vivo pore size estimation in white matter with double wave vector diffusion weighting, in: Proceedings of the International Society for Magnetic Resonance in Medicine, 18th Annual Meeting, Stockholm, Sweden, 2010, p. 194.
[17] E. Özarslan, P.J. Basser, Microscopic anisotropy revealed by NMR double pulsed field gradient experiments with arbitrary timing parameters, J. Chem. Phys. 128 (2008) 154511.
[18] M.A. Koch, J. Finsterbusch, Numerical simulations of double wave vector diffusion experiments, Magn. Reson. Med. 62 (2009) 247–254.
[19] J. Finsterbusch, Extension of the double-wave-vector diffusion-weighting experiment to multiple concatenations, J. Magn. Reson. 198 (2009) 174–182.
[20] M. Lawrenz, J. Finsterbusch, Double-wave-vector diffusion-weighting experiments with multiple concatenations at long mixing times, J. Magn. Reson. 206 (2010) 112–119.
[21] J. Finsterbusch, M.A. Koch, A tensor approach to double wave vector diffusion-weighting experiments on restricted diffusion, J. Magn. Reson. 195 (2008) 23–32.
[22] W.H. Press, S. Teukolsky, W.T. Vetterling, B.P. Flannery, Numerical Recipes in C: The Art of Scientific Computing, second ed., Cambridge University Press, Cambridge, Great Britain, 1992.
[23] R. Kimmlingen, E. Eberlein, M. Gebhardt, B. Hartinger, R. Ladebeck, R. Lazar, T. Reese, J. Riegler, F. Schmitt, G.A. Sørensen, V. Wedeen, L.L. Wald, An easy to exchange high-performance head gradient insert for a 3T whole-body MR system: first results, in: Proceedings of the International Society for Magnetic Resonance in Medicine, 12th Annual Meeting, Kyoto, Japan, 2004, p. 1630.